

# SLC17A9 expression levels in a pan-cancer panel and validation of the role of SLC17A9 as a novel prognostic biomarker for osteosarcoma

JUNQING LI<sup>1</sup>, FEIRAN WU<sup>1</sup>, LI SU<sup>1</sup>, HUIMIN ZHU<sup>1</sup>, JIE YAO<sup>1</sup> and MENG ZHANG<sup>2</sup>

<sup>1</sup>Minimally Invasive Spinal Surgery Center, Luoyang Orthopedic-Traumatological Hospital of Henan Province (Henan Provincial Orthopedic Hospital), Zhengzhou, Henan 450018;

<sup>2</sup>Department of Orthopedics, Henan Provincial People's Hospital, Zhengzhou University People's Hospital, Henan University People's Hospital, Zhengzhou, Henan 450003, P.R. China

Received November 25, 2022; Accepted April 19, 2023

DOI: 10.3892/ol.2023.13969

**Abstract.** Previous studies have demonstrated the involvement of the solute carrier family 17 member 9 (*SLC17A9*) in certain types of cancer; however, the precise role of *SLC17A9* is not well defined. In the present study, a comprehensive analysis was performed to determine the involvement of *SLC17A9* in a pan-cancer panel. First, data on *SLC17A9* expression levels from publicly available databases were obtained to determine *SLC17A9* expression profiles in various types of cancer. Next, the involvement of *SLC17A9* in the prognosis of patients, stemness indices and the immune microenvironment was examined in 34 types of cancer. Furthermore, CCK-8 and colony-formation assays were performed to determine the effect of *SLC17A9* on osteosarcoma (OSS) cells. In a pan-cancer panel, a difference in *SLC17A9* expression levels was observed in the tumor tissues as compared with healthy tissues. Furthermore, survival analysis revealed a significant association between *SLC17A9* expression levels and the prognosis of patients with various cancer types, including adrenocortical carcinoma, kidney renal clear cell carcinoma, glioblastoma, kidney renal papillary cell carcinoma, low grade glioma, liver hepatocellular carcinoma, mesothelioma, lung adenocarcinoma, skin cutaneous melanoma, uveal melanoma,

stomach adenocarcinoma and OSS. The results of the present study revealed correlations between stemness indices, tumor immunity and *SLC17A9* expression levels. Furthermore, univariate and multivariate Cox regression analyses indicated that *SLC17A9* may be utilized as an independent risk factor for overall survival of patients with OSS. *In vitro* experiments demonstrated that *SLC17A9* promotes the proliferation and viability of OSS cells. Taken together, the results of the present study suggest an association between *SLC17A9* and the prognosis of patients as well as tumor immunity in various cancer types. *SLC17A9* may serve as a novel prognostic biomarker and target for improving the prognosis of patients with OSS.

## Introduction

Solute carrier family 17 member 9 (*SLC17A9*) is localized in lysosomes and its gene encodes for a vesicular nucleotide transporter protein, a member of the transmembrane protein family (1). It is involved in small molecule transportation in cells, specifically the active transport of ATP to lysosomes. Therefore, *SLC17A9* dysfunction reduces ATP accumulation in the lysosomes, leading to cell death (1). Furthermore, studies have demonstrated that *SLC17A9* is critically involved in cell viability and the physiology of lysosomes (1,2).

In colorectal cancer, a correlation was observed between enhanced *SLC17A9* expression levels and a number of clinical as well as pathological characteristics of patients. In addition, the overall survival (OS) and disease-free survival of patients with colorectal cancer expressing high *SLC17A9* levels in tumor tissues were poor (3). Studies have demonstrated that the survival of patients with gastric cancer expressing high *SLC17A9* levels was poor (4,5). *SLC17A9* affects liver hepatocellular carcinoma (LIHC) progression. It is involved in the infiltration of immune cells into tumors and ferroptosis. Furthermore, a decrease in *SLC17A9* expression levels inhibited the proliferation, migration and colony formation of HepG2 cells (6). By contrast, low *SLC17A9* expression promotes prostate cancer cell proliferation, migration and invasion, and inhibits cell apoptosis (7). Taken together, this indicates the involvement of *SLC17A9*

---

*Correspondence to:* Professor Jie Yao, Minimally Invasive Spinal Surgery Center, Luoyang Orthopedic-Traumatological Hospital of Henan Province (Henan Provincial Orthopedic Hospital), 100 Yongping Road, Zhengzhou, Henan 450018, P.R. China  
E-mail: yaojie110120@163.com

Professor Meng Zhang, Department of Orthopedics, Henan Provincial People's Hospital, Zhengzhou University People's Hospital, Henan University People's Hospital, 7 Weiwu Road, Zhengzhou, Henan 450003, P.R. China  
E-mail: zhangmeng.lh@163.com

**Key words:** solute carrier family 17 member 9, pan-cancer, prognosis, stemness, tumor immunity, osteosarcoma

in cancer; however, its influence on the prognosis of patients has remained elusive.

Therefore, in the present study, the *SLC17A9* expression levels were examined in 34 types of cancer. Next, the association between *SLC17A9* expression levels and the prognosis of patients, stemness indices, immunity and drug sensitivity in these types of cancer were determined. Finally, Cell Counting Kit-8 (CCK-8) and colony-formation assays were performed to determine the effect of *SLC17A9* expression levels on osteosarcoma (OSS) cells. The results of the present study indicated that *SLC17A9* may serve as a prognostic marker and a therapeutic target for OSS.

## Materials and methods

*SLC17A9* expression levels in a pan-cancer panel. Standardized pan-cancer data were retrieved from databases including The Cancer Genome Atlas (TCGA), Therapeutically Applicable Research to Generate Effective Treatments (TARGET) and Genotype-Tissue Expression using the University of California Santa Cruz (UCSC) genome browser database (<https://xenabrowser.net/datapages/>) (8,9). The abbreviations used for 34 types of cancer are presented in Table SI. The data on the *SLC17A9* expression pattern in all samples were extracted and plotted using the R software. However, the data on *SLC17A9* expression levels in corresponding healthy tissues for certain types of cancer from TCGA were missing. Thus, data on the *SLC17A9* expression levels in these types of cancer and corresponding healthy tissues, including adrenocortical carcinoma (ACC), lymphoid neoplasm diffuse large B-cell lymphoma (DLBC), acute myeloid leukemia (LAML), low grade glioma (LGG), ovarian serous cystadenocarcinoma, skin cutaneous melanoma (SKCM), testicular germ cell tumors (TGCT), thymoma (THYM), and uterine carcinosarcoma (UCS), were obtained from the Gene Expression Profiling Interactive Analysis (GEPIA; <http://gepia.cancer-pku.cn/>) database (10).

*Analysis of the association between SLC17A9 expression levels and survival of patients with cancer.* To determine the association between *SLC17A9* expression and survival outcomes of various types of cancer, the OS, progression-free survival (PFS) and disease-specific survival (DSS) data of patients were obtained from the TCGA and TARGET cohorts. TCGA data including expression data and clinical data were obtained from the University of California, Santa Cruz (UCSC) database, which is an open, public database (<https://xenabrowser.net/datapages/>). In the UCSC database, not all tumor types contained the three survival times (OS, PFS, and DSS), some cancer types only contained OS or PFS. Survival analysis was performed using the Kaplan-Meier (KM) method with the median of *SLC17A9* expression as the cut-off value and the survival curves were plotted using the survival package in R. In addition, only when P was less than 0.05 can the survival curves be graphed. Next, a univariate Cox regression analysis was performed using the forestplot R package to determine the association between *SLC17A9* expression levels and survival. In addition, the association between *SLC17A9* expression levels and the survival of patients in the immunotherapy cohort was determined using KM

plotter (<https://kmplot.com/analysis/>) (11). The detailed steps were as follows: i) Enter the KM plotter website and select the 'start KM plotter for immunotherapy' button; ii) enter the gene symbol 'SLC17A9' and select the cut-off value 'median'; and iii) select survival 'OS or PFS', select follow-up threshold 'all', select Anti-PD-L1 treatment 'all', select tumor type 'all, bladder...'. .

*Analysis of the stemness index.* Stemness refers to the self-renewal and dedifferentiation properties of cells, which aid in the progression and invasion of cancer cells, thus resulting in poor prognosis of the patient (12). The two independent stemness indices are the mRNA expression-based stemness index (RNAss), which demonstrates gene expression, and the DNA methylation-based stemness index (DNAss), which reflects epigenetic features. The stemness scores of the patients were obtained from the TCGA cohort based on the UCSC database. The correlation between *SLC17A9* expression levels and the stemness indices was determined by Spearman correlation analysis.

*Analysis of tumor immunity.* The tumor microenvironment (TME) serves a crucial role in cancer progression. The proportion of stromal and immune cells in the TME of patients was determined from the TCGA cohort by calculating the estimation of stromal and immune cells in malignant tumor tissues using expression data (ESTIMATE) score (13) determined with the ESTIMATE algorithm (<https://bioinformatics.mdanderson.org/public-software/estimate/>). In addition, the cell-type identification by estimating relative subsets of RNA transcripts (CIBERSORT) tool (<https://cibersortx.stanford.edu/>) was used to determine the infiltration status of tumor-infiltrating immune cells (TIICs) in 34 types of cancer (14). Subsequently, the effect of *SLC17A9* expression on the TME and TIICs was determined.

*Drug activity analysis.* To predict potential drugs targeting *SLC17A9*, the correlation between *SLC17A9* expression levels and drug sensitivity was determined by Pearson's correlation coefficient. Furthermore, the CellMiner database (<https://discover.nci.nih.gov/cellminer/>) was examined to obtain data on drug activity (15).

*Gene Ontology (GO), Kyoto Encyclopedia of Genes and Genomes (KEGG) pathway enrichment and gene set variation analyses (GSVA).* The clusterProfiler R package (16) was employed to perform the GO and KEGG pathway enrichment analyses to determine the functions and pathways enriched by *SLC17A9*. Next, the GSVA R package (17) was used to estimate the variations in key gene sets in patients with OSS.

*Cell culture and transfection.* OSS cells were obtained from The Cell Bank of Type Culture Collection of The Chinese Academy of Sciences. U2OS, Saos2, MG63 and HOS cells were cultured in Dulbecco's Modified Eagle's Medium supplemented with 10% fetal bovine serum (both from Biological Industries), and 143 B cells were cultured in Modified Eagle's Medium (Biological Industries) supplemented with 10% fetal bovine serum. All cells were incubated at 37°C in a humidified atmosphere containing 5% CO<sub>2</sub>. GV492 was

used as the vector for overexpression and empty plasmid, and *SLC17A9* overexpression (OE) and empty (NC) vectors were constructed and provided by Shanghai GeneChem Co., Ltd. Small interfering RNAs (siRNAs) targeting *SLC17A9* (si-1, stB0012921A and si-2, stB0012921B) and negative control siRNA (si-nc, siN0000001-1-5) were designed and synthesized by Guangzhou RiboBio Co., Ltd. The si-1 and si-2 target sequences are presented in Table SII. These vectors or siRNAs were separately transfected into cells with the aid of Lipofectamine 3000 (Invitrogen; Thermo Fisher Scientific, Inc.) or riboFECT CP Transfection Kit (cat. no. C10511-05; Guangzhou RiboBio Co., Ltd). HOS and MG63 ( $1 \times 10^6$ /well) cells were seeded into a 6-well plate. After 24 h, vectors and Lipofectamine 3000 (or siRNAs and riboFECT CP reagent) were mixed and left at room temperature for 15 min, then the mixture was added to each well of the 6-well plate. MG63 cells were transfected with 5  $\mu$ g vector in each well. HOS cells were transfected with 100 nM siRNA per well. The transfected cells were incubated for 48 h at 37°C in a humidified atmosphere containing 5% CO<sub>2</sub>, and then used in subsequent experiments.

**Reverse transcription-quantitative PCR (RT-qPCR) and western blotting (WB).** RT-qPCR and WB were performed as described previously (18). RT-qPCR reagents such as AG RNAex Pro Reagent, SYBR Green Premix Pro Taq HS qPCR kit and the Evo M-MLV RT Premix kit were purchased from Accurate Biology. The sequences of the primers used are presented in Table SII. The reagents used to perform WB, including RIPA buffer and BeyoECL Plus kit, were purchased from Beyotime Institute of Biotechnology. Furthermore, anti-GAPDH (1:1,000; cat. no. 10494-1-AP) and anti-*SLC17A9* (1:500; cat. no. 26731-1-AP) antibodies were purchased from Wuhan Sanying Biotechnology, and the HRP-conjugated Affinipure Goat Anti-Rabbit IgG antibody (1:1,000; cat. no. SA00001-2) was purchased from Proteintech Group, Inc (Wuhan Sanying Biotechnology).

**Cell-proliferation and colony-formation assays.** The proliferation of cells was determined using the CCK-8 assay (Beyotime Institute of Biotechnology) following the manufacturer's protocols. For this assay,  $2 \times 10^3$  cells/well were seeded and cultured in a 96-well plate at 37°C for 0, 24, 48 and 72 h. For the colony-formation assay, 1,000 cells/well were seeded and incubated in a 6-well plate and incubated for 14 days, with the media being changed every 2 days. Next, the colonies were stained at room temperature with 1% crystal violet for 20 min. The colonies that had formed (colonies with  $\geq 50$  cells) were manually counted under a microscope.

**Statistical analysis.** Bioinformatics and statistical analyses, such as the normalization and transformation of RNA sequencing data, and the correlation, survival, CIBERSORT, ESTIMATE, GSEA, GO and KEGG analyses, were performed using the R software (version 4.0.0; <https://www.r-project.org/>). Furthermore, the coxph algorithm of the survival R package was used to perform univariate and multivariate Cox regression analyses. Pearson correlation analysis was performed to determine the correlation between *SLC17A9* expression levels and the activity of the drugs from the CellMiner database. All quantitative data from *in vitro* experiments are expressed as

the mean  $\pm$  standard deviation of three independent experiments. One-way analysis of variance followed by Tukey's post hoc test was performed using the GraphPad Prism 8.0 Software (Dotmatics) to determine differences across groups. A two-tailed  $P < 0.05$  was considered to indicate a statistically significant difference.

## Results

***SLC17A9* expression levels in pan-cancer panel.** The differences in *SLC17A9* expression profiles between pan-cancer tumor and normal samples were analyzed after obtaining data of the *SLC17A9* expression profiles for pan-cancer using publicly available data. A significant increase in *SLC17A9* expression levels was observed in 15 types of cancer (Fig. 1A and B), including LUAD, COAD, BRCA, KIRP, DLBC, head and neck squamous cell carcinoma (HNSC), LAML, KIRC, LIHC, BLCA, READ, STAD, LUSC, THCA and UCEC. However, a significant decrease in *SLC17A9* expression levels was observed in the tissues of patients with ACC (Fig. 1B).

**Significance of *SLC17A9* expression levels in predicting the prognosis of patients.** Univariate Cox regression and survival analyses were performed to determine the association between *SLC17A9* expression levels and the prognosis of patients in 34 types of cancer. The univariate Cox regression analysis demonstrated that *SLC17A9* expression was an independent prognostic factor associated with the OS of patients with various types of cancer, such as OSS, ACC, LGG, KIRC, MESO, KIRP, SKCM and UVM (Fig. 2A). Furthermore, the KM analysis demonstrated that patients with high *SLC17A9* expression and types of cancer such as KIRC, LGG, OSS or UVM had a reduced OS duration compared with patients with low *SLC17A9* expression. On the contrary, the OS duration of patients with high *SLC17A9* expression levels and BRCA was increased compared with that of patients with low *SLC17A9* expression levels (Fig. S1).

The *SLC17A9* expression levels were an independent risk factor for DSS in patients with types of cancer such as KIRC, ACC, KIRP, LGG, MESO, LIHC, SKCM, LUAD, STAD and UVM (Fig. 2B). KM analysis demonstrated that the DSS duration of patients with high *SLC17A9* expression levels and KIRC, LGG or UVM was reduced compared with that of patients with low *SLC17A9* expression levels. However, the DSS duration of patients with high *SLC17A9* expression levels and LUAD was increased compared with that of patients with low *SLC17A9* expression levels (Fig. S1). Forest plots demonstrated a significant association between *SLC17A9* expression levels and the PFS of patients with glioblastoma (GBM), LGG, KIRC, LUAD, PRAD, THYM, STAD and UVM (Fig. 2C). In addition, KM analysis demonstrated that the PFS duration of patients with high *SLC17A9* expression levels and KIRC, LGG, PRAD or UVM was reduced compared with that of patients with low *SLC17A9* expression levels (Fig. S1). The DSS and PFS of patients with high *SLC17A9* expression levels and LUAD were increased compared with those of patients with low *SLC17A9* expression levels.

The association between the *SLC17A9* expression levels and the prognosis of patients from the immunotherapy cohort

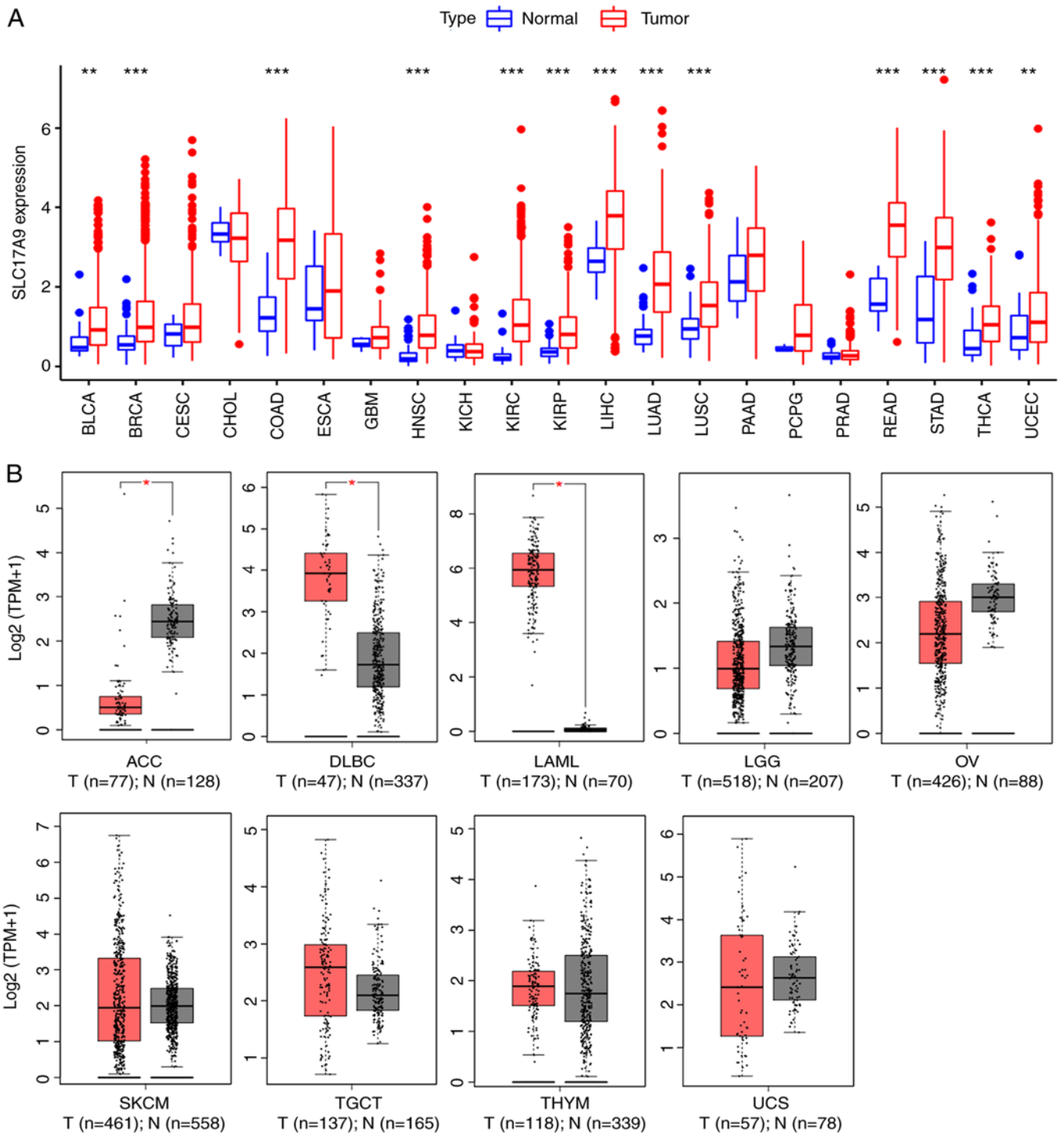


Figure 1. Analysis of *SLC17A9* expression levels in a pan-cancer panel. (A) Differential expression of *SLC17A9* in normal and tumor tissues of patients from pan-cancer TCGA cohorts. (B) *SLC17A9* expression levels in tumor tissues (red) of patients from the TCGA cohort and normal tissues (grey) from the TCGA and Genotype-Tissue Expression cohorts. \* $P < 0.05$ , \*\* $P < 0.01$  and \*\*\* $P < 0.001$ . *SLC17A9*, solute carrier family 17 member 9; TCGA, the Cancer Genome Atlas; T, tumor tissue samples; TPM, transcripts per million; N, normal tissue samples.

was also investigated using the KM plotter web-based tool. The results revealed that in several types of cancer, including bladder cancer, esophageal adenocarcinoma, GBM, hepatocellular carcinoma, melanoma, HNSC, non-small cell lung cancer, non-squamous lung carcinoma and urothelial cancer, the OS of patients with high *SLC17A9* expression levels in the antibody directed against programmed cell death-1 ligand 1 (anti-PD-L1) therapy cohort was increased (Fig. S2A).

Furthermore, a significant association was observed between the *SLC17A9* expression levels and the OS of patients with bladder carcinoma (Fig. S2B) in the anti-PD-L1 therapy cohort. Thus, *SLC17A9* may be a potential prognostic marker for various types of cancer.

*Analysis of stemness indices and tumor immunity.* The correlation between the stemness indices and the *SLC17A9* expression

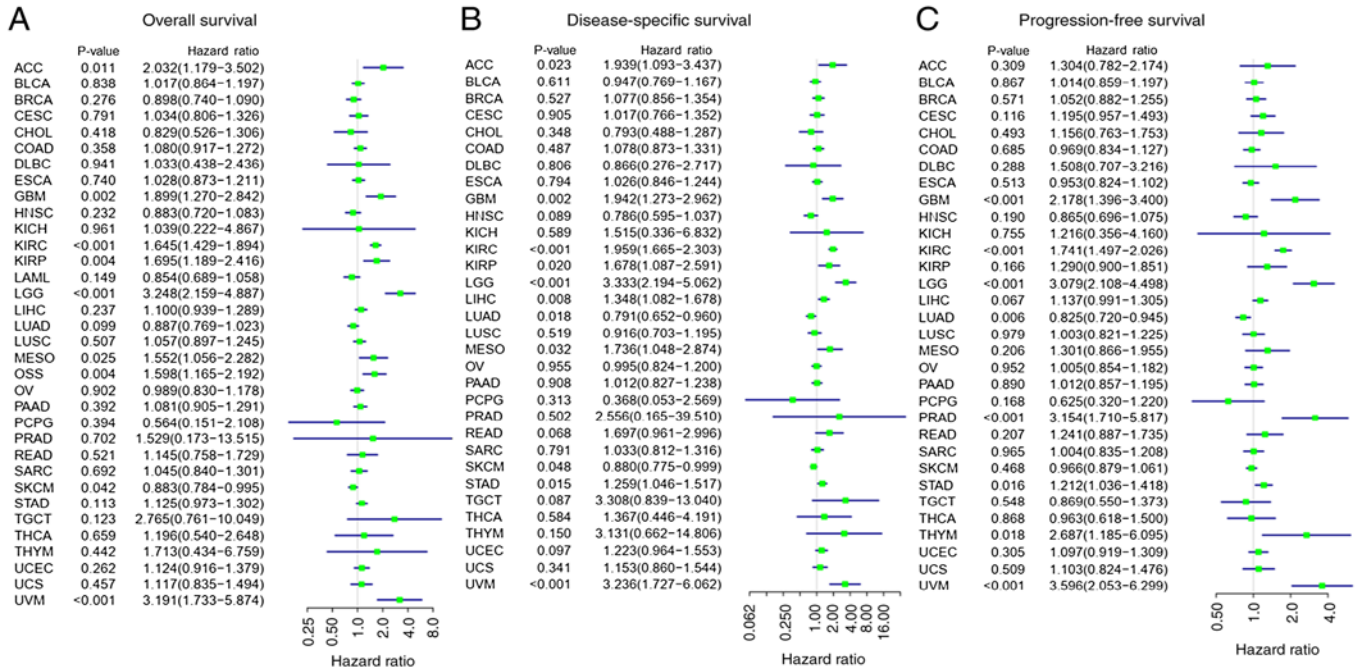


Figure 2. Forest plots demonstrating the prognostic value of solute carrier family 17 member 9 expression levels in patients in 34 types of cancer, including (A) overall survival, (B) disease-specific survival and (C) progression-free survival.

levels exhibited differences among various cancer types. A negative correlation was revealed between *SLC17A9* expression levels and the RNAss stemness index in various types of cancer, such as ACC, CESC, GBM, BLCA, HNISC, KICH, LUAD, KIRP, KIRC, LUSC, PCPG, LGG, PRAD, TGCT, SKCM and THCA. However, a positive correlation was observed between *SLC17A9* expression levels and the RNAss stemness index in other types of cancer, such as PAAD and STAD (Fig. 3A). In addition, the *SLC17A9* expression level was negatively correlated with the DNAss stemness index in BLCA, CESC, LAML and TGCT, and positively correlated in other types of cancer, such as HNISC, BRCA, KIRC, LGG, MESO, KIRP, PAAD, THCA, PRAD, SARC, PCPG, STAD and UVM (Fig. 3A).

The ESTIMATE algorithm was used to calculate the stromal and immune scores of patients. A positive correlation was observed between the *SLC17A9* expression levels and the immune score of patients with BRCA, KIRC, GBM, ACC, HNISC, ESCA, UCEC, KIRP, LGG, KICH, SKCM, LUAD, BLCA, MESO, OSS, PCPG, SARC, LUSC, TGCT, PRAD, THYM, THCA and UVM. However, a negative correlation was observed between the *SLC17A9* expression level and the immune score of patients with COAD, LAML, PAAD and STAD (Fig. 3B). Furthermore, the results revealed a positive correlation between the *SLC17A9* expression level and the stromal scores of patients with ACC, BLCA, ESCA, ESCA, KICH, GBM, HNISC, KIRP, LGG, LUSC, MESO, PRAD, SKCM, TGCT, THYM, SARC, THCA and UCEC. However, a negative correlation was observed between the *SLC17A9* expression level and the stromal scores of patients with LAML, OSS, PAAD and STAD (Fig. 3B). Taken together, these results suggest a significant correlation between the *SLC17A9* expression level and stemness indices such as RNAss and DNAss, as well as the immune and stromal scores of patients with BLCA, HNISC, LGG, PAAD, TGCT, PRAD, KIRP, STAD and THCA.

Next, whether there was a correlation between *SLC17A9* expression and the levels of 22 types of TIIC was determined. The results demonstrated a positive correlation between *SLC17A9* expression and nine TIICs, including plasma cells, naïve and memory B cells, memory-activated CD4 T cells, resting natural killer (NK) cells, regulatory T (Treg) cells, M0 macrophages, eosinophils and neutrophils. On the contrary, a negative correlation was observed between *SLC17A9* expression levels and the levels of other types of immune cell, such as naïve CD4 T cells, activated NK cells, T follicular helper (Tfh) cells, monocytes, M1 and M2 macrophages, resting and activated dendritic cells, and activated mast cells (Fig. 3C). Furthermore, differences in TIIC levels were observed among patients with different types of cancer. In patients with ACC or DLBC, there was a strong positive correlation between the *SLC17A9* expression levels and immune cells such as neutrophils and resting NK cells, respectively. Furthermore, *SLC17A9* expression levels were revealed to be positively correlated with resting memory CD4 T cells in ESCA and to be negatively correlated with monocytes in LAML. In patients with PRAD, THYM or UVM, there was a positive correlation between the *SLC17A9* expression levels and immune cells such as Treg cells, plasma cells and M1 macrophages, respectively (Fig. 3C). However, no significant correlation was observed between *SLC17A9* expression levels and the infiltration of 22 immune cell types in patients with BLCA or UCS (Fig. 3C). These results indicate a correlation between the *SLC17A9* expression level and the degree of immune-cell infiltration in different types of cancer.

*SLC17A9* enhances OSS cell proliferation and viability. In the dataset GSE16088, an increase in *SLC17A9* expression levels was observed in the tissues of patients with OSS compared with those in healthy bone tissues (Fig. 4A). Furthermore, in

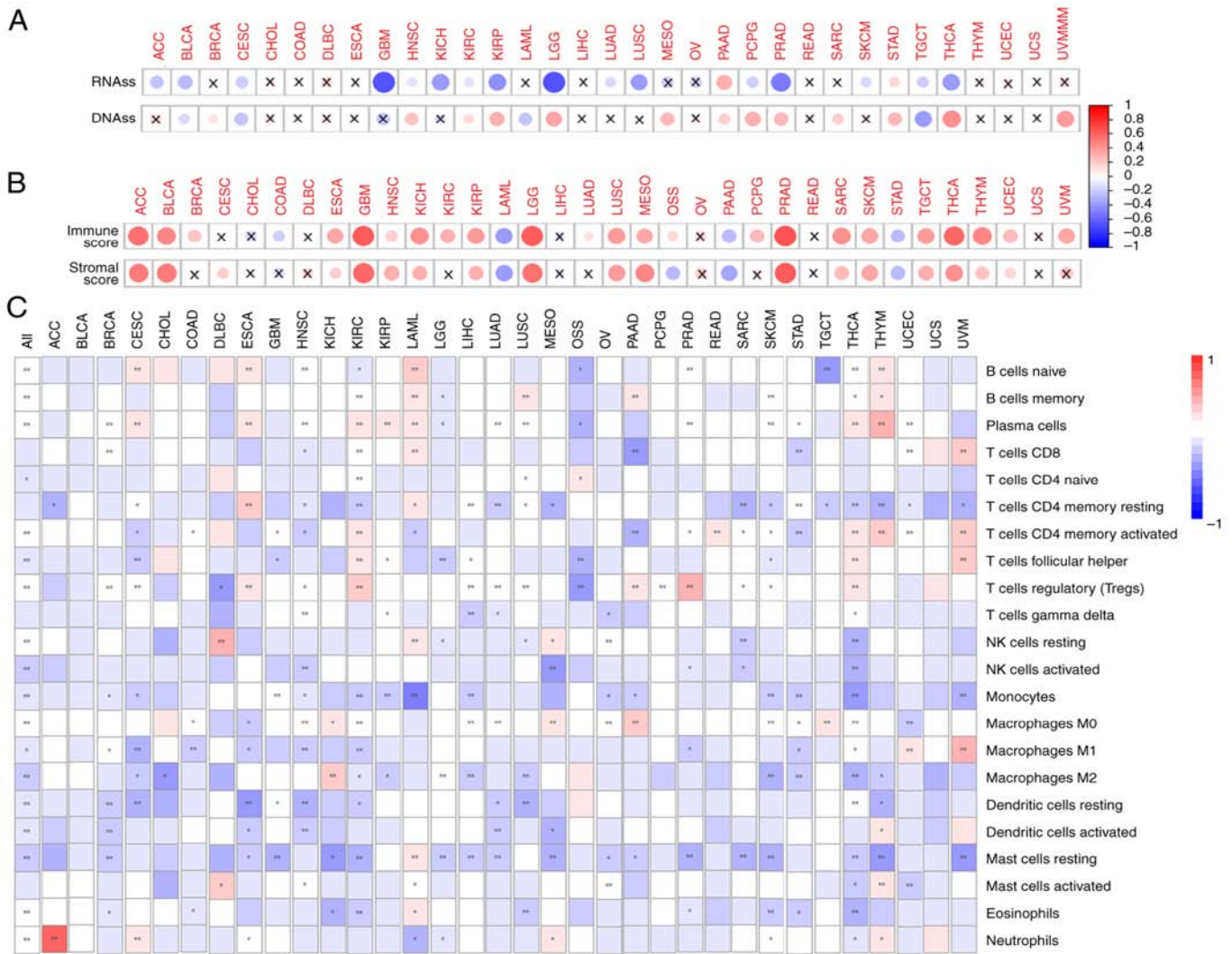


Figure 3. Correlation between solute carrier family 17 member 9 expression levels and (A) stemness indices, (B) tumor microenvironment and (C) tumor-infiltrating immune cells in a cancer panel. \* $P > 0.05$ , \* $P < 0.05$  and \*\* $P < 0.01$ . RNAss, mRNA expression-based stemness index; DNAss, DNA methylation-based stemness indices; NK, natural killer.

the TCGA-TARGET dataset, the OS (Figs. 4B and S1) and relapse-free survival (Fig. 4B) of patients with high *SLC17A9* expression levels were poor compared with those of patients with low *SLC17A9* expression levels. Univariate and multivariate Cox regression analyses of the TCGA-TARGET dataset demonstrated that *SLC17A9* may be an independent risk factor for the OS of patients with OSS (Fig. 4C).

Next, RT-qPCR was performed to determine *SLC17A9* expression levels in several OSS cell lines (Fig. 4D). HOS and MG63 cells were used for the subsequent experiments since *SLC17A9* levels were high in HOS and low in MG63 cells. HOS cells were transfected with siRNAs (si-nc, si-1 and si-2) and MG63 cells were transfected with *SLC17A9*-NC or *SLC17A9*-OE vectors. Finally, RT-qPCR and WB analyses were performed to confirm the knockdown and overexpression of *SLC17A9* in HOS and MG63 cells, respectively (Fig. 4E). The results of the CCK-8 assay revealed a decrease in the proliferation capacity of *SLC17A9*-knockdown HOS cells (si-1 or si-2) compared with cells transfected with si-NC. In addition, there was an increase in the proliferation of MG63 cells transfected with the *SLC17A9*-OE vector compared

with the cells transfected with *SLC17A9*-NC (Fig. 4F). The colony-formation assays indicated a considerable reduction in the colony number of HOS cells with *SLC17A9* knockdown, while there was a substantial increase in the colony numbers of MG63 cells overexpressing *SLC17A9* (Fig. 4G). These results indicate that *SLC17A9* has a role to enhance the proliferation and viability of OSS cells. Thus, *SLC17A9* may be significantly involved in enhancing OSS progression.

*GSEA and GO and KEGG pathway enrichment analyses.* Next, GO and KEGG pathway enrichment analyses were performed to determine the functions and pathways enriched by *SLC17A9* in OSS. Fig. 5A reveals that *SLC17A9* was enriched in biological processes such as ossification, connective tissue and cartilage development, the bone morphogenetic protein signaling pathway and odontogenesis. In addition, *SLC17A9* was enriched in cellular component terms such as the collagen-containing extracellular matrix. The molecular function terms enriched by *SLC17A9* were extracellular matrix structural constituents, receptor serine/threonine kinase and TGF- $\beta$  receptor binding, growth factors activity,

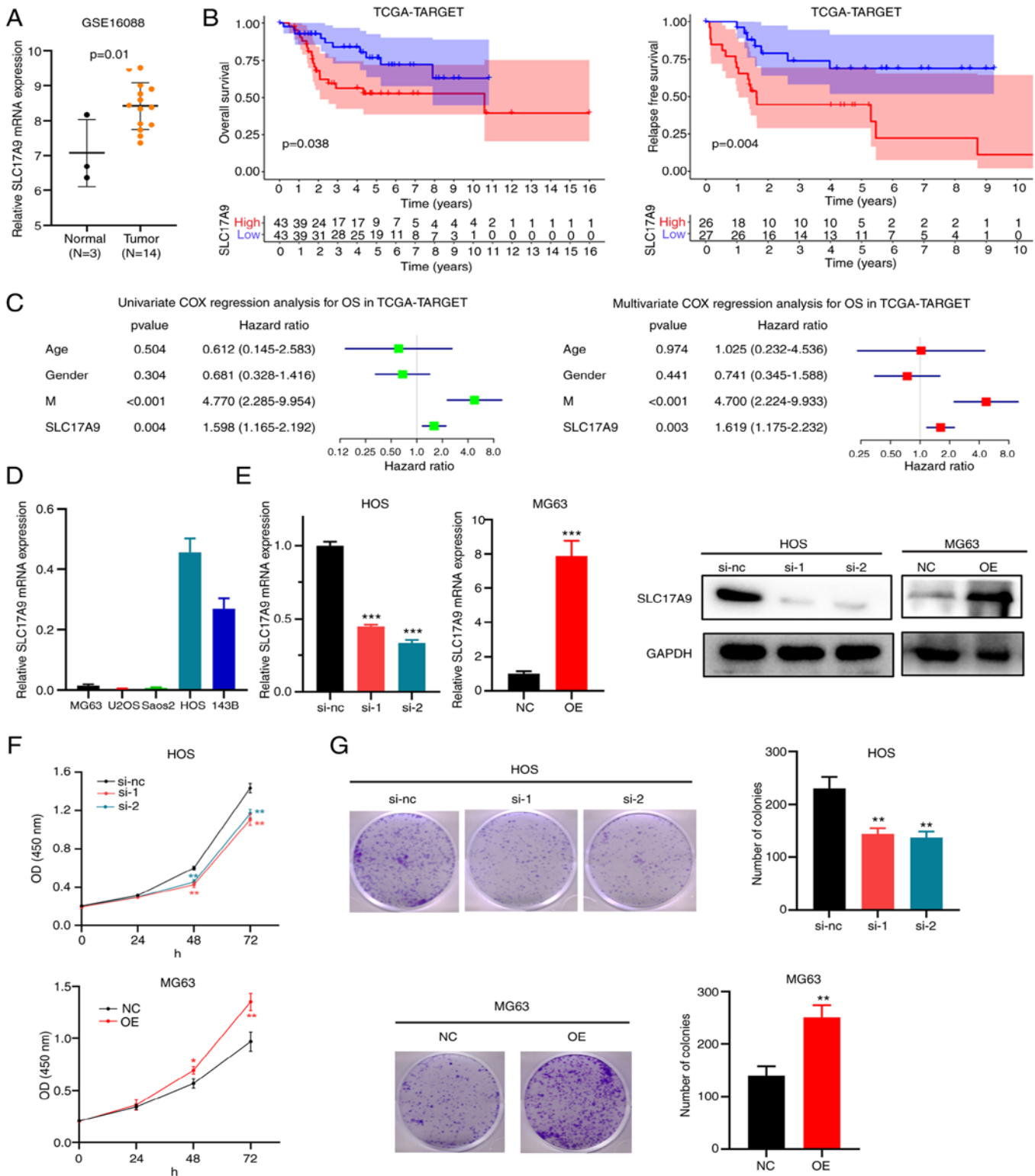


Figure 4. Cellular functions of *SLC17A9* in OSS. (A) Differential expression of *SLC17A9* in tumor tissues compared with normal tissues in OSS (accession no. GSE16088). (B) Association between high *SLC17A9* expression levels and poor OS and relapse-free survival of patients from the TCGA-TARGET cohort. (C) Univariate and multivariate Cox regression analysis of the OS of patients from the TCGA-TARGET cohort. (D) *SLC17A9* expression levels in OSS cells. (E) *SLC17A9*-knockdown HOS cells and *SLC17A9*-OE MG63 cells were constructed. Reverse transcription-PCR and western blot analysis were used to determine *SLC17A9* expression levels in these cells. (F) Effect of *SLC17A9* on the proliferation of HOS and MG63 cells. (G) Effect of *SLC17A9* on the viability of HOS and MG63 cells. \*\*P<0.01 and \*\*\*P<0.001 vs. NC. *SLC17A9*, solute carrier family 17 member 9; M, metastasis; OSS, osteosarcoma; OS, overall survival; TCGA, The Cancer Genome Atlas; TARGET, Therapeutically Applicable Research to Generate Effective Treatments; si-nc, negative control small interfering RNA; si-1/2, small interfering RNA targeting *SLC17A9*; NC, empty overexpression vector; OE, overexpression; OD, optical density.

racemase and epimerase activity. The KEGG pathway enrichment analysis demonstrated that *SLC17A9* was enriched

in the MAPK, Hippo, focal adhesion and TGF- $\beta$  signaling pathways (Fig. 5B). Finally, GSVA was performed to compare

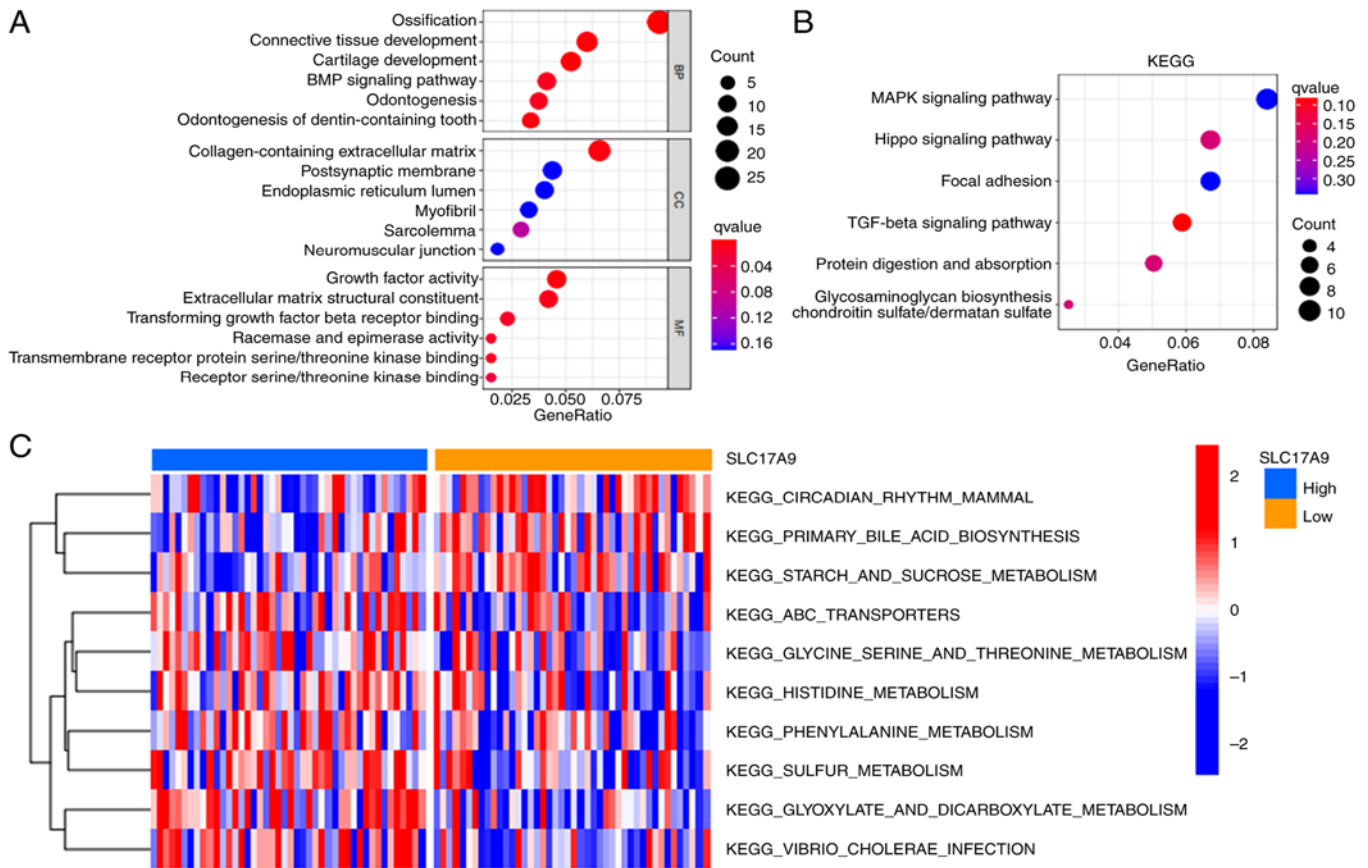


Figure 5. GSVA and the GO and KEGG pathway enrichment analyses. (A) The GO and (B) KEGG pathway enrichment analyses of *SLC17A9*. (C) GSVA was performed on patients with osteosarcoma with low and high *SLC17A9* expression levels from the Cancer Genome Atlas-Therapeutically Applicable Research to Generate Effective Treatments cohort. *SLC17A9*, solute carrier family 17 member 9; KEGG, Kyoto Encyclopedia of Genes and Genomes; GO, Gene Ontology; CC, cellular component; BP, biological process; MF, molecular function; GSVA, gene set variation analyses; BMP, bone morphogenetic protein.

the pathways enriched in patients with OSS with high or low *SLC17A9* expression levels. The GSVA results revealed significant differences in pathways such as circadian rhythm in mammals, starch and sucrose metabolism, ABC transporters, glycine serine/threonine, histidine, phenylalanine, sulfur, glyoxylate and dicarboxylate metabolism and *Vibrio cholerae* infection between the high and low expression groups (Fig. 5C).

**Drug sensitivity analysis.** Data on 263 anticancer drugs were retrieved from the CellMiner database. Next, Pearson correlation analysis was performed to determine the correlation between *SLC17A9* expression levels and the activity of these drugs in NCI-60 cells (15). The scatterplot in Fig. 6 revealed the correlation analysis results: A positive correlation was observed between *SLC17A9* expression levels and the sensitivity to drugs such as vorinostat, asparaginase, chelerythrine, hypothemycin, PX-316, entinostat, acrichine, LDK-378 and imexon. A negative correlation was observed between *SLC17A9* expression levels and the sensitivity to drugs including ibrutinib, afatinib and sonidegib.

## Discussion

A previous study has demonstrated the involvement of *SLC17A9*, a transmembrane protein, in small-molecule

transportation (1). Furthermore, *SLC17A9* controls ATP accumulation in lysosomes, thus altering cell survival (1). Recent studies have demonstrated that *SLC17A9* has a role in cancer development (6,7). In LIHC, *SLC17A9* acts as a tumor promoter gene that influences tumor progression (6). In PRAD, *SLC17A9* acts as a tumor suppressor that attenuates proliferation, apoptosis and metastasis of cancer cells (7). However, the role of *SLC17A9* in other types of cancer has remained elusive. Therefore, in the present study, *SLC17A9* expression levels were comprehensively analyzed in a pan-cancer panel. Next, the impact of *SLC17A9* on patient prognosis, tumor immunity and stemness was determined in various types of cancer. Finally, the functions of *SLC17A9* were verified in OSS cells.

The results of the present study revealed an increase in *SLC17A9* expression levels in the tumor tissues of 15 types of cancer, including COAD (3), STAD (4) and LIHC (6,19). However, a decrease in *SLC17A9* expression levels was observed in ACC tissues. In addition, a significant difference in the status of methylation of the *SLC17A9* promoter was observed in tumor tissues compared with normal tissues in 14 types of cancer. Extensive perturbations in DNA methylation alter the expression levels of genes regulating tumorigenesis, thus affecting the progression of cancer and the prognosis of the patient (20). These results indicate the involvement of *SLC17A9* in the onset and progression of different types of cancer.



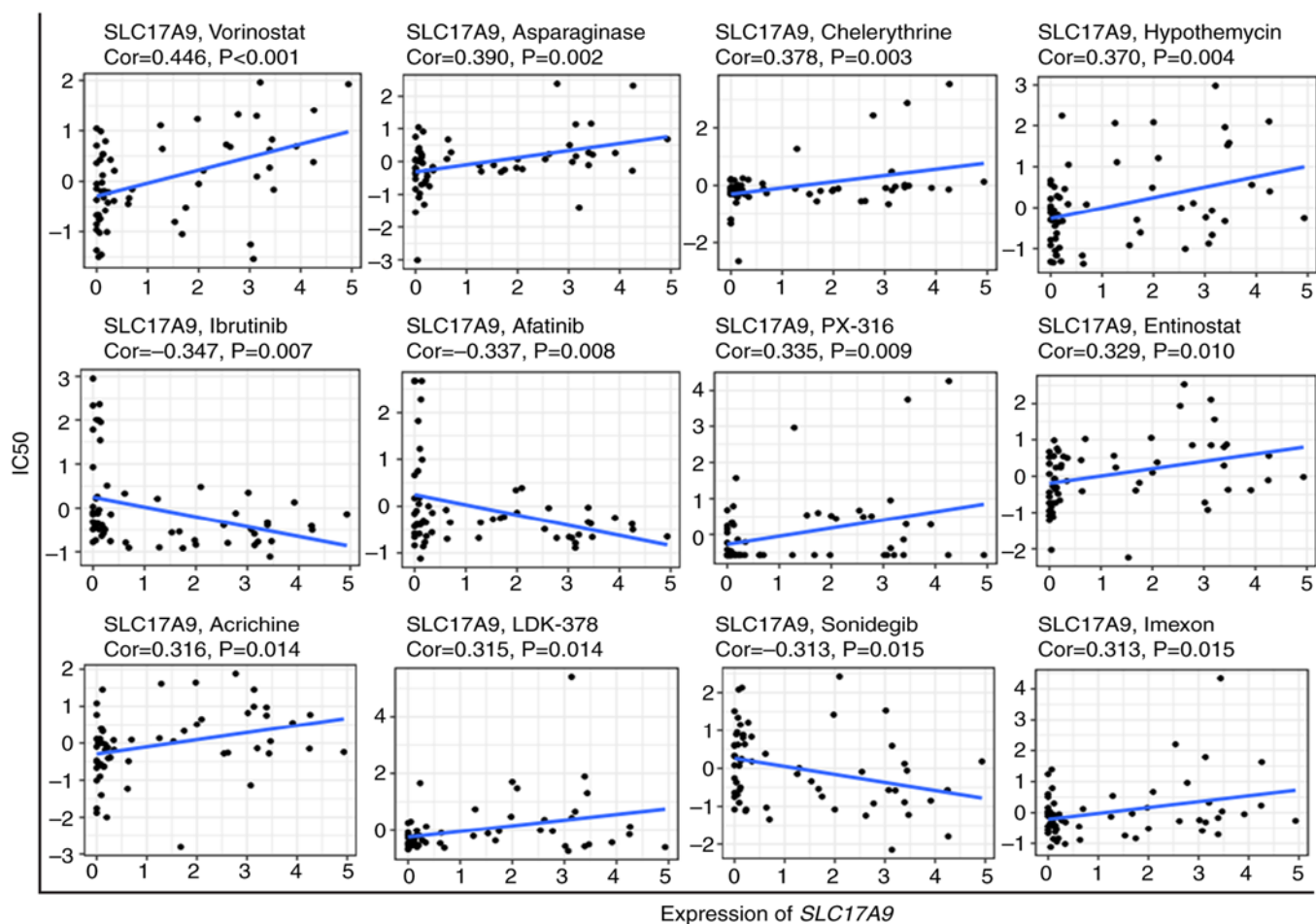


Figure 6. Correlation between *SLC17A9* expression levels and expected drug response in NCI-60 cells from the CellMiner database. *SLC17A9*, solute carrier family 17 member 9; Cor, correlation coefficient.

Survival analysis for multiple types of cancer was performed using univariate Cox regression analysis and the KM method. The results revealed an association between *SLC17A9* expression levels and the prognosis of patients with various types of cancer, including COAD (3), STAD (4,5), LIHC (6,19) and KIRC (21), consistent with previous studies. A correlation was observed between high *SLC17A9* expression levels and longer PFS and DSS of patients with LUAD. *SLC17A9* was able to suppress tumorigenesis in LUAD and PRAD (7). In the anti-PD-L1 therapy cohort, high *SLC17A9* expression levels were associated with an increase in the OS of patients. Therefore, the potential mechanisms by which *SLC17A9* affects anti-PD-L1 treatment are worth investigating. These results suggest that *SLC17A9* may be a promising prognostic marker in various tumor types.

A previous study has demonstrated a close association between stemness, the status of cancer progression and metastasis and poor prognosis of patients in a pan-cancer panel (12). Therefore, the association between *SLC17A9* expression levels and the two stemness indices was investigated. A significant association was observed between *SLC17A9* expression levels and RNAss in 18 types of cancer, including GBM, LGG and PRAD. In addition, a significant association was observed between *SLC17A9* expression levels and DNAss in 17 types of cancer, including TGCT, THCA and UVM. Furthermore, these

stemness indices were associated with intratumor heterogeneity, immune microenvironment and immune response (12). Therefore, the role of *SLC17A9* in different types of cancer should be further investigated.

Previous studies have demonstrated that the TME serves a significant role in tumor onset and progression; thus, targeting the TME appears to be a promising approach in the treatment of cancer (22,23). First, the results of the present study indicated a significant difference in the *SLC17A9* expression levels in six immune subtypes of 13 types of cancer. Next, the stromal and immune scores were calculated to determine the status of the TME of patients. The results of the present study indicated a positive correlation between the *SLC17A9* expression levels and the stromal scores in 18 types of cancer, as well as the immune scores in 23 types of cancer. However, a significant negative correlation was observed between the *SLC17A9* expression levels and the stromal as well as the immune scores of patients with LAML, PAAD and STAD.

In addition, the results of the present study demonstrated a significant correlation between the *SLC17A9* expression levels and the infiltration of immune cells in 32 types of cancer. The results of the present study indicated a negative correlation between the *SLC17A9* expression levels and the immune cells such as Tfh and Treg cells in patients with OSS. Tfh cells express high PD1 levels and are closely associated with

antitumor immunity. In addition, Tfh-like cells are present in several types of cancer (24). A previous study has revealed the synergistic effect of combining therapies targeting Treg cells and other treatment strategies (25). These results suggest synergistic immunotherapy may be used to target *SLC17A9* for treating patients with OSS.

However, the role of *SLC17A9* in cancer remains controversial. Therefore, *in vitro* experiments were performed using OSS cells to determine the functions of *SLC17A9*. The results suggested that *SLC17A9* enhances OSS cell proliferation and viability. Next, the underlying mechanisms of *SLC17A9* were investigated. The KEGG pathway enrichment analysis indicated that *SLC17A9* was enriched in the MAPK, Hippo, focal adhesion and TGF- $\beta$  signaling pathways. Furthermore, several known drugs targeting *SLC17A9* were identified.

Of note, the present study has certain limitations. First, data were obtained, analyzed and integrated from several publicly available databases, which primarily included patients of Caucasian ethnicity. This may cause bias due to ethnicity. Furthermore, the *SLC17A9* protein significantly influences the occurrence and progression of cancer; therefore, it is necessary to determine the effect of *SLC17A9* protein expression in multiple types of cancer. In addition, the underlying mechanisms of the role of *SCL17A9* remain to be elucidated. Thus, additional studies should be performed to design new *SLC17A9*-based therapeutic strategies for improving patient survival.

In conclusion, the results of the present study demonstrate that *SCL17A9* was differentially expressed and significantly associated with tumor immunity as well as the prognosis of patients with various types of cancer. It was demonstrated that *SLC17A9* functions as a tumor promoter in OSS. *SLC17A9* may be a novel prognostic biomarker and a potential target for synergistic immunotherapy of OSS.

#### Acknowledgements

Not applicable.

#### Funding

No funding was received.

#### Availability of data and materials

All data generated or analyzed during this study are included in this published article.

#### Authors' contributions

MZ and JY conceptualized and supervised the study. JL performed the bioinformatic analysis and statistical analysis. MZ performed the *in vitro* experiments. FW, LS and HZ performed the data curation and interpretation. JL wrote the original manuscript. MZ and JY confirm the authenticity of all the raw data. All authors read and approved the final version of the manuscript.

#### Ethics approval and consent to participate

Not applicable.

#### Patient consent for publication

Not applicable.

#### Competing interests

The authors declare that they have no competing interests.

#### References

1. Cao Q, Zhao K, Zhong XZ, Zou Y, Yu H, Huang P, Xu TL and Dong XP: *SLC17A9* protein functions as a lysosomal ATP transporter and regulates cell viability. *J Biol Chem* 289: 23189-23199, 2014.
2. Huang P, Cao Q, Xu M and Dong XP: Lysosomal ATP Transporter *SLC17A9* controls cell viability via regulating cathepsin D. *Cells* 11: 887, 2022.
3. Yang L, Chen Z, Xiong W, Ren H, Zhai E, Xu K, Yang H, Zhang Z, Ding L, He Y, *et al*: High expression of *SLC17A9* correlates with poor prognosis in colorectal cancer. *Hum Pathol* 84: 62-70, 2019.
4. Li J, Su T, Yang L, Deng L, Zhang C and He Y: High *SLC17A9* expression correlates with poor survival in gastric carcinoma. *Future Oncol* 15: 4155-4166, 2019.
5. Sun M, Qiu J, Zhai H, Wang Y, Ma P, Li M and Chen B: Prognostic implications of novel gene signatures in gastric cancer microenvironment. *Med Sci Monit* 26: e924604, 2020.
6. Kui XY, Gao Y, Liu XS, Zeng J, Yang JW, Zhou LM, Liu XY, Zhang Y, Zhang YH and Pei ZJ: Comprehensive analysis of *SLC17A9* and its prognostic value in hepatocellular carcinoma. *Front Oncol* 12: 809847, 2022.
7. Mi YY, Sun CY, Zhang LF, Wang J, Shao HB, Qin F, Xia GW and Zhu LJ: Long Non-coding RNAs LINC01679 as a competitive endogenous RNAs inhibits the development and progression of prostate cancer via regulating the miR-3150a-3p/*SLC17A9* axis. *Front Cell Dev Biol* 9: 737812, 2021.
8. Goldman MJ, Craft B, Hastie M, Repečka K, McDade F, Kamath A, Banerjee A, Luo Y, Rogers D, Brooks AN, *et al*: Visualizing and interpreting cancer genomics data via the Xena platform. *Nat Biotechnol* 38: 675-678, 2020.
9. Blum A, Wang P and Zenklusen JC: SnapShot: TCGA-Analyzed tumors. *Cell* 173: 530, 2018.
10. Tang Z, Li C, Kang B, Gao G, Li C and Zhang Z: GEPIA: A web server for cancer and normal gene expression profiling and interactive analyses. *Nucleic Acids Res* 45(W1): W98-W102, 2017.
11. Lánckzy A and Györfly B: Web-Based survival analysis tool tailored for medical research (KMplot): Development and implementation. *J Med Internet Res* 23: e27633, 2021.
12. Malta TM, Sokolov A, Gentles AJ, Burzykowski T, Poisson L, Weinstein JN, Kamińska B, Huelsken J, Omberg L, Gevaert O, *et al*: Machine learning identifies stemness features associated with oncogenic dedifferentiation. *Cell* 173: 338-354. e15, 2018.
13. Yoshihara K, Shahmoradgoli M, Martínez E, Vegesna R, Kim H, Torres-Garcia W, Treviño V, Shen H, Laird PW, Levine DA, *et al*: Inferring tumour purity and stromal and immune cell admixture from expression data. *Nat Commun* 4: 2612, 2013.
14. Newman AM, Liu CL, Green MR, Gentles AJ, Feng W, Xu Y, Hoang CD, Diehn M and Alizadeh AA: Robust enumeration of cell subsets from tissue expression profiles. *Nat Methods* 12: 453-457, 2015.
15. Reinhold WC, Sunshine M, Liu H, Varma S, Kohn KW, Morris J, Doroshow J and Pommier Y: CellMiner: A web-based suite of genomic and pharmacologic tools to explore transcript and drug patterns in the NCI-60 cell line set. *Cancer Res* 72: 3499-3511, 2012.
16. Yu G, Wang LG, Han Y and He QY: clusterProfiler: An R package for comparing biological themes among gene clusters. *OMICS* 16: 284-287, 2012.
17. Hänzelmann S, Castelo R and Guinney J: GSVA: Gene set variation analysis for microarray and RNA-seq data. *BMC Bioinformatics* 14: 7, 2013.
18. Li J, Su L, Xiao X, Wu F, Du G, Guo X, Kong F, Yao J and Zhu H: Development and validation of novel prognostic models for immune-related genes in osteosarcoma. *Front Mol Biosci* 9: 828886, 2022.

19. Wu J, Yang Y and Song J: Expression of SLC17A9 in hepatocellular carcinoma and its clinical significance. *Oncol Lett* 20: 182, 2020.
20. Hao X, Luo H, Krawczyk M, Wei W, Wang W, Wang J, Flagg K, Hou J, Zhang H, Yi S, *et al*: DNA methylation markers for diagnosis and prognosis of common cancers. *Proc Natl Acad Sci USA* 114: 7414-7419, 2017.
21. Meng M, Lan T, Tian D, Qin Z, Li Y, Li J and Cao H: Integrative bioinformatics analysis demonstrates the prognostic value of chromatin accessibility biomarkers in clear cell renal cell carcinoma. *Front Oncol* 11: 814396, 2021.
22. Xiao Y and Yu D: Tumor microenvironment as a therapeutic target in cancer. *Pharmacol Ther* 221: 107753, 2021.
23. Roma-Rodrigues C, Mendes R, Baptista PV and Fernandes AR: Targeting tumor microenvironment for cancer therapy. *Int J Mol Sci* 20: 840, 2019.
24. Crotty S: T follicular helper cell biology: A decade of discovery and diseases. *Immunity* 50: 1132-1148, 2019.
25. Li C, Jiang P, Wei S, Xu X and Wang J: Regulatory T cells in tumor microenvironment: New mechanisms, potential therapeutic strategies and future prospects. *Mol Cancer* 19: 116, 2020.



Copyright © 2023 Li et al. This work is licensed under a Creative Commons Attribution-NonCommercial-NoDerivatives 4.0 International (CC BY-NC-ND 4.0) License.